A Real-Time Vibrational Spectroscopic Investigation of the Low-Temperature Oscillatory Regime of the Reaction of NO with CO on Pt{100}

J. H. Miners,[†] P. Gardner,[‡] A. M. Bradshaw,[†,||] and D. P. Woodruff*[,§]

Fritz-Haber-Institut der Max-Plank-Gesellschaft, Faradayweg 4-6, D-14195 Berlin, Germany, Department of Chemistry, Faraday Building, The University of Manchester Institute of Science and Technology, Manchester M60 1QD, U.K., and Department of Physics, The University of Warwick, Coventry CV4 7AL, U.K.

Received: August 21, 2003

A new experimental method for obtaining real-time in situ infrared reflection−absorption spectra of any reproducibly reversible process has been applied to reveal the time-dependent coverages of adsorbates during the low-temperature oscillatory regime of the NO + CO reaction on Pt{100}. Simultaneous acquisition of real-time mass spectrometry data is used to relate the coverages to the rates of reaction, providing new insight into the mechanisms involved in the oscillation. NO and CO are shown to be present at estimated coverages varying between 0.06 and 0.20 monolayers (ML) for CO and between 0.27 and 0.36 ML for NO at different points in the cycle. The relative phases of these two coverage oscillations differ very significantly. CO is present in both atop and bridging geometries, but the two species exhibit identical adsorption and reaction behavior, attributed to the high rate of equilibration between the two configurations. Overall, the results show strong similarities to the predictions of the well-established model of Fink et al. (*J. Chem. Phys.* **1991**, *95*, 2109), but there are also notable differences. The results indicate a significant role for the nonreactive displacement of NO by CO not included in this model. Some of the other discrepancies may relate to unavoidable surface inhomogeneity associated with reaction front propagation at key points in the oscillatory cycle such as the "surface explosion" involving coadsorbed NO and CO. The coexistence of nonreacting CO poisoned islands are also found to occur at the lowest temperatures.

1. Introduction

Kinetic oscillations in the catalytic oxidation of CO were discovered more than 30 years ago in experiments performed over polycrystalline Pt surfaces at atmospheric pressure.[1−3] More recent studies, in particular on the CO + O_2 and CO + NO reactions, have focused on single-crystal surfaces, where the full arsenal of modern surface science techniques can be applied.[4,5] Single-crystal surface studies at low pressure (P_{tot} < 10^{-4} mbar) also offer some important simplifications. For example, the adsorbed species can be expected to occupy specific positions in a well-defined two-dimensional array and one has very good control over the external parameters of temperature and partial and total pressure and can ensure homogeneity of all these parameters. The work of the Ertl group, in particular, has revealed a variety of phenomena known from other nonlinear systems, such as the transition to chaos, chemical waves, and the formation of Turing structures and of complex spatio-temporal patterns.[6,7]

In the NO + CO reaction on Pt{100}, which we discuss here, it is now well established that, using a mixture of NO and CO with a partial pressure ratio in the range 0.8 > P_{NO}−P_{CO} > 1.8, there are two distinct temperature regimes which exhibit oscillatory behavior. Such reaction rate oscillations have been observed for total pressures ranging from 10^{-9} mbar on a Pt-{100} single crystal[8] to 1 bar on a polycrystalline platinum surface[7] (for which the active face is {100}). The exact temperature at which kinetic oscillations occur depends on the total pressure of the reactants. The two regimes are, however, separated by approximately 20 K and are thus generally referred to as the high- and the low-temperature oscillatory regimes.[9] Low-energy electron diffraction (LEED) measurements have shown that the rate oscillations in the high-temperature oscillatory regime occur on a partially reconstructed surface, with the transformation between the reconstructed "hex" surface phase (the equilibrium clean surface structure at room temperature in which the surface layer adopts a hexagonal close-packed arrangement) and a nominally ideally terminated (1 × 1) surface playing an important role in the bistability, whereas the surface is entirely in the (1 × 1) phase in the low-temperature oscillatory regime.[9]

Fink et al. have modeled the reaction mathematically and have reproduced the steady-state behavior and the lower temperature kinetic oscillations, by assuming adsorbate island formation and a vacant site requirement for NO dissociation. The individual steps in the mechanism are shown schematically in Figure 1.[9] Briefly, these are as follows: In step I, the surface is composed of intermixed NO and CO having a high coverage which inhibits NO dissociation due to lack of suitable vacant sites. In this state, a chance desorption event leads to the creation of a vacant site, allowing an adsorbed NO to dissociate, forming atomic O and atomic N; the atomic O reacts with a CO molecule to form CO_2 and the atomic N combines with another N to form N_2. Both of these products desorb, thus creating more vacant surface sites upon which NO can dissociate. The resulting exponential

* Corresponding author. E-mail: D.P.Woodruff@Warwick.ac.uk.
[†] Fritz-Haber-Institut der Max-Plank-Gesellschaft.
[‡] The University of Manchester Institute of Science and Technology.
[§] The University of Warwick.
[||] Present address: Max-Planck-Insititut für Plasmaphysik, Boltzmannstrasse 2, D-85748 Garching, Germany.

10.1021/jp036487q CCC: $27.50
Published on Web 01/08/2004

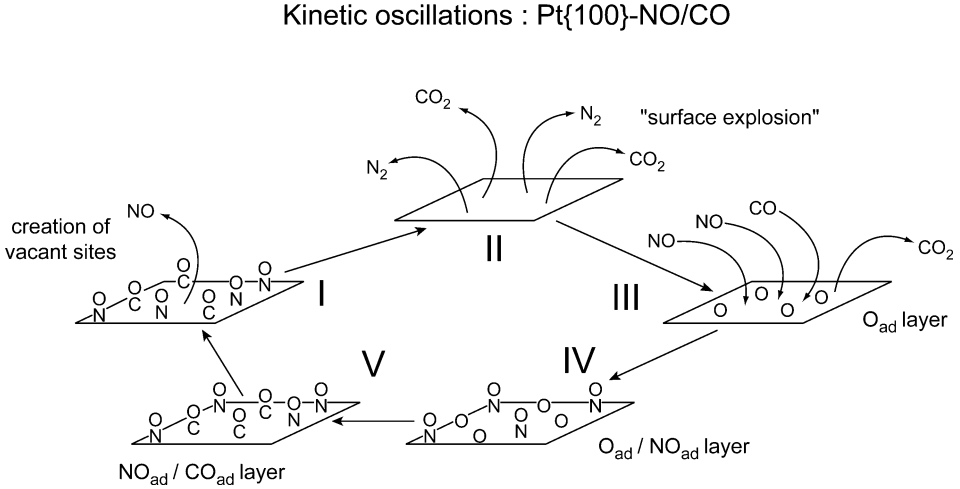

Figure 1. Schematic diagram of mechanism for the low-temperature NO + CO oscillatory reaction on Pt{100} proposed by Fink et al.[9]

creation of vacant surface sites leads to the so-called surface explosion (step II), which rapidly reduces the surface coverage by a factor of 2. Recently, Tammaro and Evans have proposed a spatio-temporal model for the development of the surface explosion and its passage, as a chemical wave, through the adsorbate layer (steps I and II).[10] In step III, any NO adsorbing on the clean areas of the surface immediately dissociates and the atomic nitrogen produced desorbs almost immediately as N_2, but because these experiments are conducted under conditions in which the partial pressure of NO is greater than that of CO, the oxygen titrates away any excess of adsorbed CO. As the CO is removed, the surface oxygen coverage increases, eventually reaching a state in which NO dissociation is hindered, and the NO coverage increases again (step IV). The surface oxygen is then removed by reaction with impinging CO molecules (step V), allowing adsorption of NO and CO from the gas phase at the free sites created to regenerate the mixed NO + CO islands. Notice that this regeneration is almost certainly aided by a separate process, proposed by Hopkinson and King,[11] in which the CO also displaces NO nonreactively (due to its greater heat of adsorption). Although this nonreactive displacement is not included in the modeling equations used by Fink et al., the driving force for the cyclic behavior in both models is considered to be the surface explosion and the subsequent availability of vacant sites for NO dissociation. The mathematical model of Hopkinson and King[11] predicts essentially the same behavior in the lower temperature existence region but not in the upper one, where the reaction mechanism is very similar to that of the oscillatory CO + O_2 reaction on the same surface.

These models, based on specific assumptions regarding the reaction mechanisms, do appear to provide a reasonable description of the kinetics as measured experimentally by changes in the gas partial pressures. However, the more detailed predictions of these models, which relate directly to the underlying mechanisms, namely, the nature and concentration of the species adsorbed on the surface during the reaction, have not been challenged by experimental measurements. This absence of experimental data stems, of course, from the difficulty of applying many standard surface science techniques at the high partial pressures of the reactants, which are present during the reaction. In this regard, in situ optical vibrational spectroscopy (photon-in, photon-out) offers the possibility of overcoming this limitation. By use of infrared reflection−absorption spectroscopy (IRAS), the intensities, spectral frequencies (wavenumbers), and widths of the vibrational bands provide information on the nature and chemical environment of the molecular species involved.

In a separate publication, we have presented IRAS and TPR (temperature-programmed reaction spectroscopy) measurements of the temperature dependence of NO and CO coadsorption behavior on Pt{100} hex and shown that it is determined by three processes,[12] which also define the parameter space of the two oscillatory regimes. At temperatures below those at which NO dissociation (and thus reaction) occurs (below about 390−400 K), the adsorption behavior is principally determined by the nonreactive displacement of preadsorbed NO by CO, attributed to the 0.23 eV greater heat of adsorption of CO.[13] This displacement initially leads to the formation of mixed NO + CO islands but eventually produces an equilibrium state comprising a CO-saturated surface (and thus a surface which is CO-poisoned from the point of view of the CO/NO reaction). At 390 K, and partial pressures of NO and CO equivalent to those under which chemical oscillations are observed, exposure to CO reduces the preabsorbed NO coverage by 50% in 30 s.[12] Above 390−400 K, NO can dissociate (providing that there are free sites available for the dissociation products), and the resulting reaction of the atomic oxygen with CO leads to desorption of CO_2 and N_2 and thus to vacant site creation. Vacant sites are preferentially filled by NO because $((s_{NO}p_{NO})/(s_{CO}p_{CO})) > 1$ under the conditions of the experiment, where s is the sticking coefficient and p is the partial pressure. The reaction therefore results in an increase in NO coverage. It is the competition between the nonreactive displacement of NO by CO and the reactive replacement of CO by NO which determines the parameter space of the low-temperature oscillatory regime and results in the formation of mixed, reacting islands of NO + CO. Coincidentally, these coadsorption studies[12] show that both bridge and atop CO species exist on the surface in dynamic equilibrium and their rapid rate of interconversion leads to the two species exhibiting identical behavior in terms of coverage changes.

While these measurements under steady-state conditions provide valuable insight into the mechanisms which underlie the CO/NO reaction over Pt{100}, a full understanding of the processes occurring within the oscillatory reaction requires truly time-dependent measurements which interrelate the adsorbate coverage and the reaction rate. The challenge to achieve this on single-crystal surfaces is to obtain sufficient sensitivity combined with a temporal resolution significantly shorter than the period of oscillation of the reaction. In principle, the rapid-scanning facility of modern Fourier transform IR spectrometers

can provide sufficient temporal resolution to follow an oscillatory cycle of the order of seconds, since a single scan at 2 cm^{-1} resolution can easily be made in 100 ms or less. In a typical surface science experiment, however, involving submonolayer adsorbate coverages, several hundred such individual interferograms must be added in order to obtain a sufficient signal−noise ratio. By degrading the spectral resolution and/or compromising the signal−noise ratio, temporal resolution can be improved but inevitably important information is lost.

Of course, the fact that the time dependence of interest is periodic means that all the measurements need not be completed in the time-scale of a single oscillation, and data recorded at equivalent times in the period cycle may be added. One possible but rather complex approach to this problem is the synchronized step-scan method, in which interferograms representing temporal resolution elements of an oscillatory cycle are constructed by adding single data points or groups of data points from successive cycles.[14] Although this method can achieve very high temporal resolution (<1 μs), it is not a viable method for the present problem. In particular, if individual data points are being added to construct an interferogram, ∼8000 oscillation cycles would be required to obtain a single interferogram of 2 cm^{-1} resolution for each temporal resolution element. Given that typical oscillation periods for the reactions of interest here are of the order of tens of seconds, the total data acquisition time is unrealistically large. Moreover, even very small variations in the oscillation period or loss of precise synchronization will lead to spectral artifacts in the final transformed interferogram.[14]

Recently, we have demonstrated the viability of a modification of this approach that offers a more realistic compromise between good temporal and spectral resolution and sensitivity, enabling detailed information regarding the coverages and local environment of the surface adsorbates, together with the partial pressures of the reactants and products, to be obtained throughout the oscillation cycle,[15] and this approach has subsequently been applied to studies of the high-temperature oscillatory regime of the NO/CO reaction on Pt{100}.[16,17] Briefly, it involves sustaining the oscillatory cycle and continuously recording interferograms over a period of many oscillatory cycles. Interferograms recorded at equivalent points in the oscillatory cycle are then added to create a single data set representing a single oscillatory period. Since whole interferograms are added, spectral artifacts are not introduced into the system and the advantage of adding data over many oscillatory periods is maintained. Notice that because IRAS samples a large area of the surface, it is important that the state of the whole surface oscillates in phase during the oscillatory reaction; typically a temperature step can trigger the oscillations, but these are damped at the low pressures used in our experiments due to loss of macroscopic synchronicity.[18,19] The application of an external global coupling mechanism, in the present case a small temperature modulation at the natural frequency of the oscillation forces a homogeneous oscillation and is not thought to change the mechanism of the reaction. The partial pressures of the reactants and products are measured simultaneously with the IR spectra so that the relative phases of the oscillations in these signals can be related to those of the infrared data from the adsorbates. Our original demonstration of this special form of time-resolved IRAS was conducted on the Pt{100}/NO + CO system, but a number of details of the results and their interpretation proved ambiguous, possibly due in part to the relatively low spectral resolution used.[15] Here we present the results of new and more extensive measurements performed at higher resolution and discuss them in the light of our more recent extensive study of the coadsorption behavior of NO and CO on Pt{100} under steady-state conditions.[12]

2. Experimental Details

The experimental procedure for collecting the time-dependent IRAS and partial-pressure measurements has been outlined above and described in more detail previously.[15] The Pt{100} sample was prepared in situ by the usual ion bombardment and annealing cycles and then cooled to a temperature 10 K above that of the existence range of the oscillatory regime to be studied. Prior to initiating the oscillations, NO was then admitted to the chamber and left to stabilize to a pressure of 7.5×10^{-7} mbar over a period of several hours. CO was then introduced such that the p_{NO}/p_{CO} ratio was 1.5. After a period of pressure stabilization (∼60 min), during which time the partial pressures of both gases were continuously monitored with the mass spectrometer, the crystal was heated to 700 K and cooled to a temperature ∼10 K above that of the existence range of the oscillatory regime to be studied. A temperature modulation of the desired period and amplitude (60 s and 2.0−2.5 K) was then applied to the sample in order to initiate and sustain the oscillations, and the mean temperature was gradually reduced until the natural frequency of the system was in resonance with the applied temperature oscillation. This condition was identified by a large increase in the amplitude of oscillation of the CO_2 partial pressure. Although this procedure is often referred to as forcing the oscillations, extensive studies of periodic and random temperature perturbations of this system have shown that it can only be forced to oscillate at frequencies very close to the natural frequency, i.e., the system acts as a narrow band-pass filter.[18]

To check that the system was behaving in the fashion determined by the natural oscillation period of the reaction, tests were conducted in which the applied temperature modulation was turned off; no change was seen in the form or period of the gas-phase partial-pressure traces, as measured by the mass spectrometer. Previous work has shown that the natural frequencies of the system at the upper and lower temperature extremes of a modulation amplitude of 2.5 K may differ by a maximum of 10%.[9] This effect can also be minimized by ensuring that the same degree of deviation from the applied frequency is exhibited at the high and the low-temperature extremes of the modulation.[17] After these checks were performed, the temperature modulation was reapplied and, following a second period of stabilization (∼10−20 min), in which the amplitude and shape of the CO_2 partial pressure oscillation had become completely reproducible, the IR data acquisition was started.

Figure 2 shows a schematic diagram of the experimental control system and data acquisition procedure. A signal generator drives the temperature controller, which periodically modulates the temperature of the sample. During the oscillations, the partial pressure of NO (30 amu), CO + N_2 (28 amu), and CO_2 (44 amu) were continuously monitored with the quadrupole mass spectrometer installed on the ultrahigh vacuum chamber. Simultaneously, the FTIR spectrometer continuously records a succession of interferograms over as many oscillatory periods as required. Notice that there is no *active* synchronization of the IR spectra collection and the reaction oscillations, but the relative timing is coordinated via the temperature of the sample. The infrared spectrometer gives out a trigger pulse each time a spectrum is acquired, which is fed into a PC. This records the spectrum number, the temperature of the sample and the time at which the spectrum was obtained. Another PC simultaneously records the temperature of the sample and the data from the mass spectrometer. Thus each data point in the mass spectrum

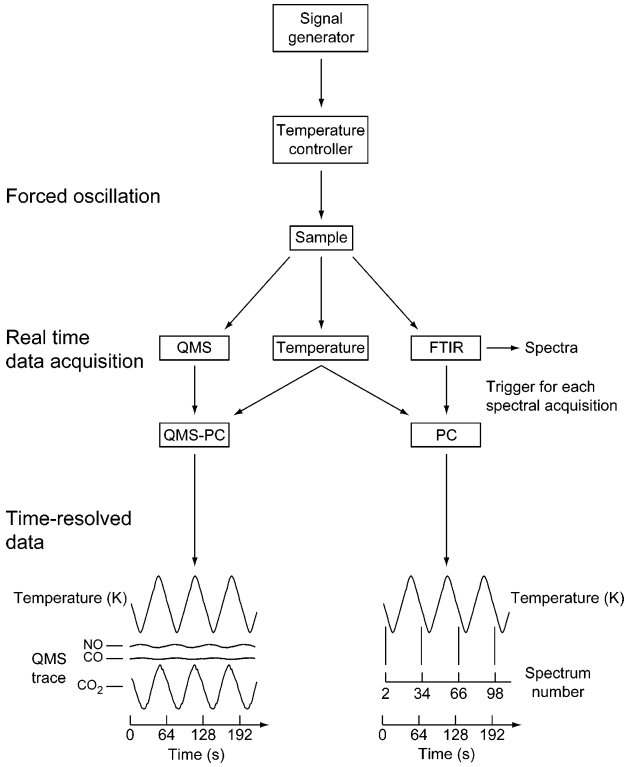

Figure 2. Schematic diagram of the control system for producing forced oscillations and synchronously measuring FTIR spectra and partial pressure data.

and each FTIR spectrum can be uniquely identified in terms of the time and temperature at which they were recorded. Spectra from equivalent points in the cycle are then combined and averaged to give a set of spectra that represent a single period of oscillation, as illustrated in Figure 2.

The temporal resolution of this method is determined by the time it takes to record a single interferogram, although in the case of the Biorad FTS 60 used here, the practical limit is the time it takes to record *two* interferograms from the forward and reverse directions of the moving mirror since these are automatically added. However, since the times at which the interferograms are collected are not actively synchronized to the reaction oscillations, the effective temporal resolution is actually twice the time required to record a single spectrum. By use of the experimental setup described here, a single spectrum resulting from the addition of a forward and a reverse interferogram takes 250 ms. In a surface science experiment, typically several hundred interferograms are added to obtain a spectrum of sufficient signal−noise ratio. Thus, using the present method, data from hundreds of oscillatory cycles would have to be added to obtain spectra of comparable quality. Given that our oscillation period is approximately 60 s, the total measurement time to achieve the best possible time resolution is thus many hours, leading to potential problems with accumulated surface contamination. It was decided to degrade the temporal resolution such that a set of spectra with a good signal−noise ratio could be acquired over 20 oscillatory cycles by taking data in blocks of 8 interferograms, giving a total of 160 interferograms in each summation (of 2 cm^{-1} resolution) recorded at 2 s intervals, giving a temporal resolution of 4 s. Figure 3 illustrates how this summation is performed, showing the individual spectra from measurements taken at an average temperature of 401.7 K at equivalent relative times in four-reaction oscillations, their sum, and the final spectrum for this relative time after summation over all 20 cycles. Notice that in these spectra the weak feature at 1750 cm^{-1} is an artifact resulting from the polarizer and a small amount of drift in the spectrometer.

3. Results and Discussion

3.1. Overview and the Role of Two Distinct Atop CO Species. Figure 4 shows the set of time-resolved IRAS spectra corresponding to 2 s intervals within a single period of oscillation of the NO + CO reaction over Pt{100}, resulting from our experiment conducted at an average temperature of 398 K within the low-temperature existence regime of the oscillatory reaction. The overall behavior is similar to that reported in the experiments conducted as part of the original demonstration of this method,[15] but there are important detailed differences, in part due to the higher spectral resolution of the present data (2 cm^{-1}) but also due to the slightly lower temperature (398 K rather than 402 K). In particular, while the main absorption bands are at 1628, 1875, and 2070 cm^{-1}, this highest wavenumber band is clearly split into two distinct components at 2065 and 2085 cm^{-1} in the new data of Figure 4. From previous infrared studies of the reactant molecules on Pt{100}, the three main bands can be assigned to the internal stretching modes of NO, bridged CO, and atop CO, while the two atop CO components can be assigned to CO in mixed NO + CO islands and CO in pure CO islands respectively.[12,20−25] Notice that the exact frequencies associated with these vibrational modes are influenced by dynamic dipole coupling, which allows us to establish the nature of the environment of the adsorbed molecules, and specifically the *local* coverage of identical species, which determines the degree of vibrational coupling. In particular, the frequencies of the 1628 cm^{-1} (NO) and 2065 cm^{-1} (atop CO) absorption bands are shifted down from those expected for pure islands of their respective individual molecular species on the same surface; this has been shown in steady-state coadsorption experiments to be associated with the formation of domains of intermixed NO + CO on Pt{100}, which results in a reduction of the dipole−dipole coupling between identical species.[26] The frequency of the bridged CO stretch is only slightly shifted from that observed when the surface is prepared in an identical manner in the absence of an applied NO partial pressure,[23] so on the basis of the frequency shifts alone it is not possible to establish whether the bridged CO is also intermixed with the NO. As we shall show, however, the variations of intensity of the atop and bridge species during the reaction cycle do clearly establish that the bridged CO is similarly intermixed. Notice, incidentally, that the frequencies of these absorption bands are all indicative of adsorption on the (1 × 1) surface, consistent with the low-temperature oscillatory reaction occurring on an entirely unreconstructed surface as has been previously established in diffraction studies.

The presence of the 2085 cm^{-1} C−O stretching mode associated with islands of pure atop CO was also found at almost the same temperature (400 K) in the steady-state experiments presented previously.[12] The interpretation in terms of pure CO islands is further reinforced by the observation that this adsorption band is much narrower than the lower frequency band associated with atop CO intermixed with NO; for this latter state, there will be a range of local environments and thus significant inhomogeneous line broadening. Figure 5 shows an overlay of the IRAS spectra in the C−O stretching range through the reaction cycle. This shows very clearly that while the absorbance of the 2065 cm^{-1} band varies strongly during the cycle, that of the 2085 cm^{-1} is constant, as is its exact peak wavenumber

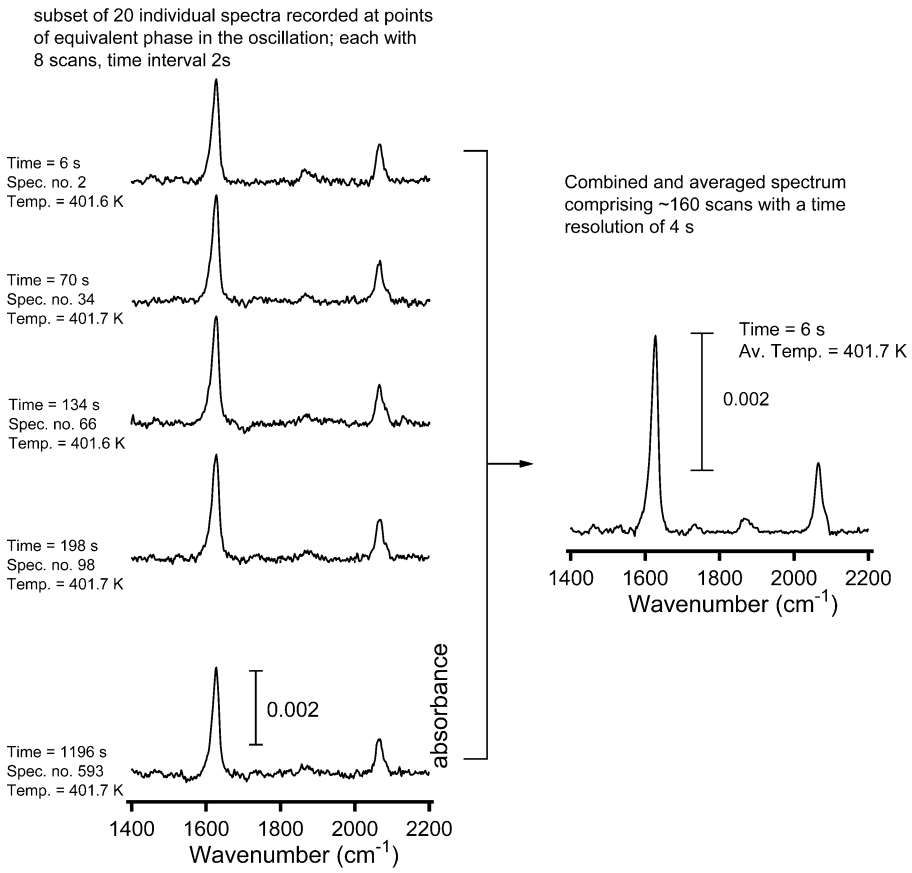

Figure 3. Illustration of how FTIR spectra, recorded at times of equivalent phase in the oscillation are combined and averaged to yield a single spectrum of increased signal-to-noise ratio. The spectra are taken from a set of measurements of the CO/NO oscillatory reaction over Pt{100} similar to those shown in Figure 4 but recorded at a slightly different temperature.

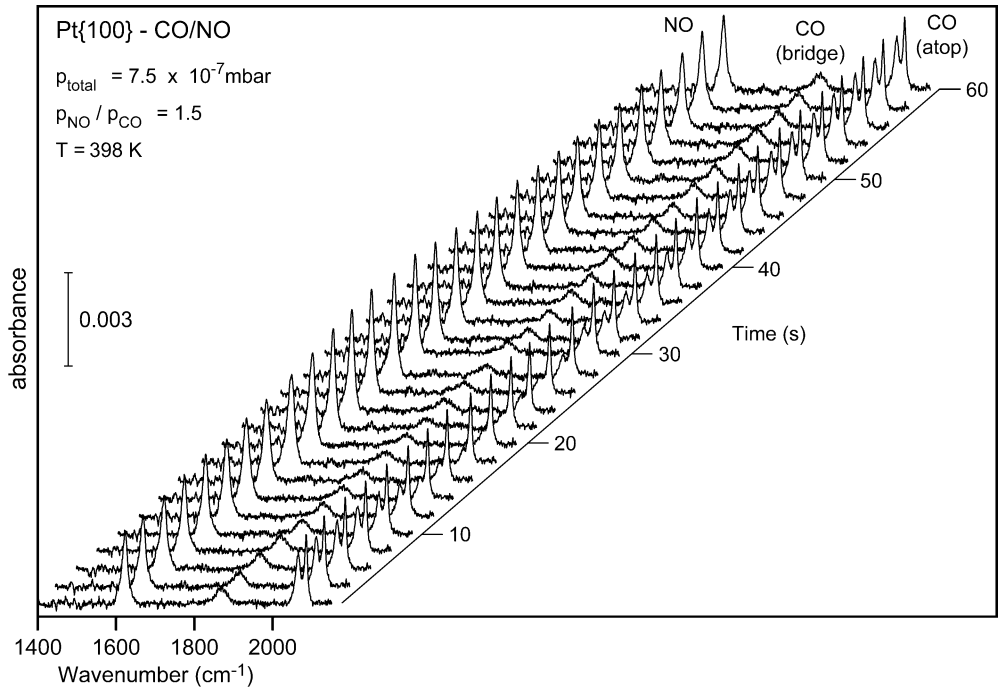

Figure 4. A series of 30 IRAS (FTIR) spectra at intervals of 2 s representing a single period in the CO/NO reaction over Pt{100} in the low-temperature oscillatory regime. Each spectrum is recorded with spectral resolution of 2 cm^{-1}, comprised of 160 scans, and represents the combination of spectra recorded over 20 oscillatory cycles, with a time resolution of 4 s (cf. Figure 3).

and width. This lack of variation implies very clearly that these pure CO islands are not involved in the oscillatory reaction. The spectra of Figure 5 also provide further evidence that the two atop CO species are spatially distinct. Because the frequencies of the two bands are very close, we would expect strong vibrational coupling to occur if the associated molecules were

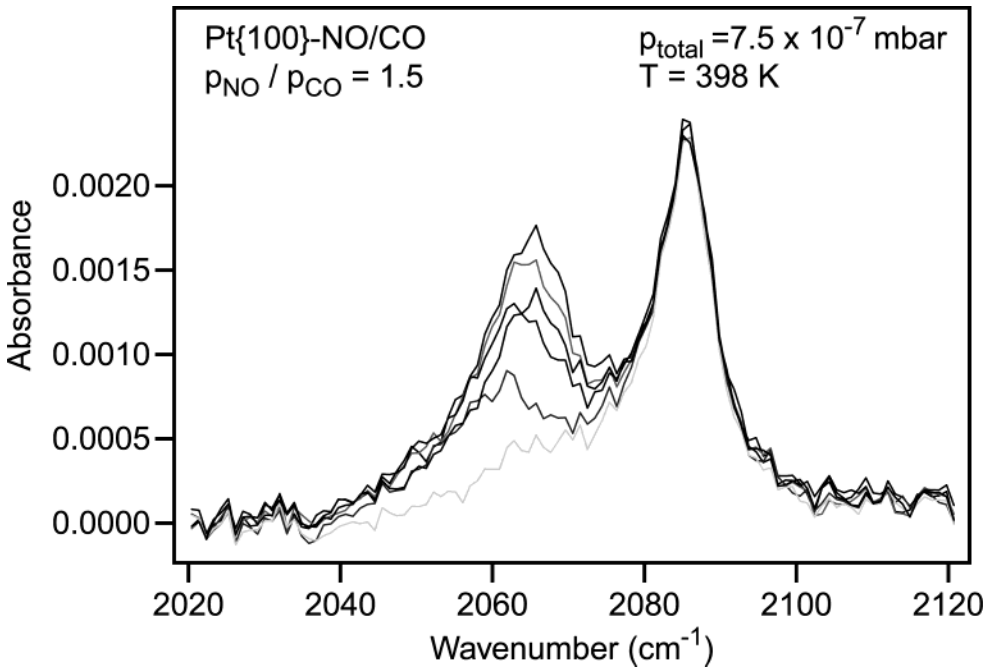

Figure 5. Overlay of an expanded section of the IRAS spectra of Figure 4 in the spectral range corresponding to the atop C−O stretching vibrations.

close to one another; this would lead to intensity transfer to the higher-frequency peak and thus to variations in its intensity due to the variations of intensity of the lower-frequency peak.

The clear evidence that the pure atop CO islands exist on the surface, not participating in the reaction, and unchanged over many cycles of the reaction on the remainder of the surface is puzzling. A completely CO-saturated surface ought to be passive because there would be no free sites for NO adsorption and dissociation, and NO arriving from the gas phase is known not to displace adsorbed CO. However, one might still have expected that reaction could occur at the edges of these islands, especially as at these high temperatures the CO is very mobile.[27,28] On the other hand, atomic oxygen produced by NO dissociation is strongly bound to the surface and is immobile at this temperature,[29,30] i.e., it cannot diffuse *into* these islands, so this might limit the edge activity. We should also stress that the relative contribution of these pure CO islands to the IRAS data was found to be very sensitive to the conditions of the experiment and especially to the temperature. Notice, for example, that in Figure 3, recorded at the same spectral resolution as the spectra of Figure 4 but an average temperature 3.7 K higher (401.7 K), the pure atop CO peak at 2085 cm^{-1} is present only as a small high-wavenumber shoulder on the peak at 2065 cm^{-1}. Much the same appears to be true of the original measurements conducted at 402 K although in view of the lower resolution it is difficult to be sure.[15] One possible underlying reason for this narrow range of mutual existence of the reacting and nonreacting regions of the surface may be related to the temperature dependence of the rate of NO dissociation, the key step in the NO/CO reaction; this is typically regarded as occurring only above about 400 K, so very close to this temperature the rate of dissociation will be delicately balanced and could be significantly influenced by some subtle property of the environment (including free sites for dissociation) at the edge of the pure CO islands.

3.2. Detailed Data Evaluation and Comparison with the Model Predictions of Fink et al. In Figure 6 is summarized the variations of the integrated absorbance of the four IRAS bands through the oscillatory reaction cycle together with the associated variations in the partial pressures at mass numbers 28 (CO + N_2), 30 (NO), and 44 (CO_2). Also shown is the temperature variation of the sample applied to ensure a spatially synchronous reaction. Since this experiment is performed under continuous flow conditions at high pumping speed, decreases in the partial pressures of reactants and increases in the partial pressures of the products are proportional to the rate of their reaction and the rate of their production, respectively. Furthermore, we anticipate that the IRAS-integrated absorbances should be linearly related to the coverage of the relevant species; this is not, of course, universally true for IRAS, and in the case of CO in Pt{100}, studies indicate that this linear relationship may be lost due to site switching and possible tilting of molecules for coverages above $\theta_{CO} = 0.5$ monolayers (ML),[22] but below this coverage the assumption is believed to be essentially valid for both NO and CO, and is consistent with previous results.[12,15]

Figure 6 shows that the form of the temporal variations of the CO_2 partial pressure is essentially identical to the negative of the NO partial pressure changes and is also clearly similar to the variation of the time derivative of the absorbance of the NO internal stretch. Unfortunately the coincidence in mass number of CO and N_2 make it difficult to deduce much detail regarding the temporal variations of these individual reactant and product species from the combined trace in Figure 6. To overcome this limitation, a separate experiment was performed using high purity $^{13}C^{18}O$ (^{13}C, 99%; ^{18}O, 98.4%), leading to a CO mass of 31 amu with a negligible contribution (0.002%) at 28 amu. TPR measurements of Zemlyanov et al. [31] show that the kinetic isotope effect in using $^{13}C^{18}O$ will not lead to a significant change in oscillatory behavior. Representative results from this additional experiment, recorded at 396 K with an applied temperature modulation of 2 K, are displayed in Figure 7. The mass spectrometer signals are averaged over 5 oscillations of 60 s; each point represents a 2.65 s segment of the oscillation with an effective time resolution of 5.3 s. The mass 31 signal ($P_{^{13}C^{18}O}$) has been corrected to remove the mass spectrometer cracking contribution of the $^{13}C^{18}O^{16}O$ signal (5.7%), and the mass 30 signal ($P_{^{14}N^{16}O}$) has been corrected to remove the $^{12}C^{18}O$ contribution, which is 1.0% of the $^{13}C^{18}O$ signal. To simplify the comparison of the different partial pressure variations, Figure

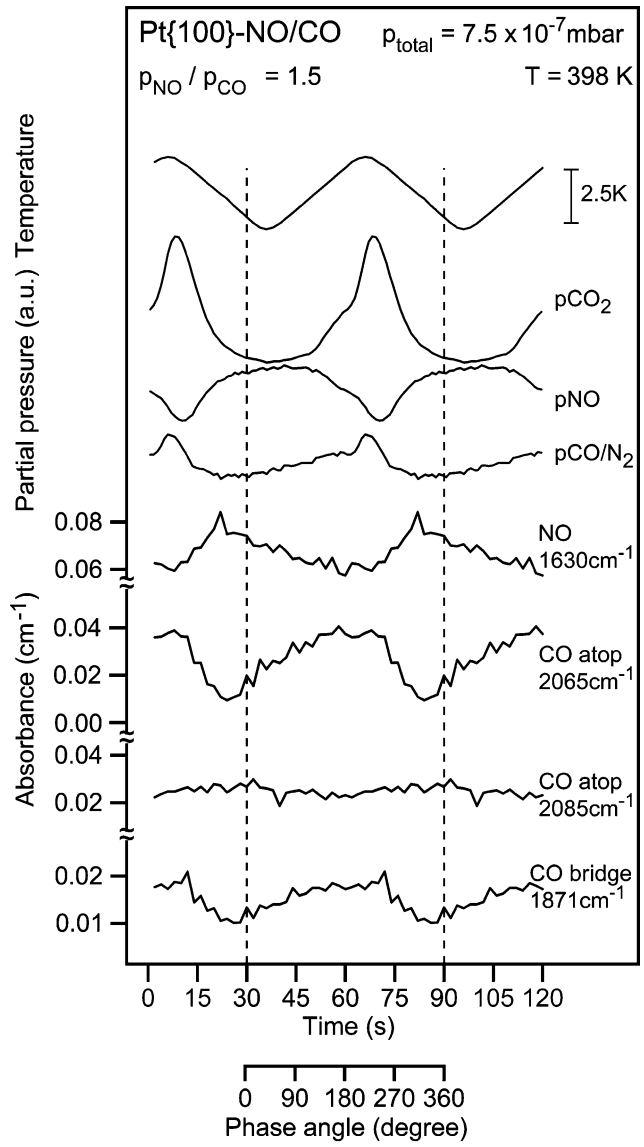

Figure 6. The time dependence of the sample temperature, CO_2, NO, and CO + N_2 partial pressures, and the integrated absorbance of the four IR absorption bands (N−O, atop C−O (2065 cm^{-1}), atop C−O (2085 cm^{-1}), and bridge C−O) during an oscillatory cycle, corresponding to the experiment of Figure 4.

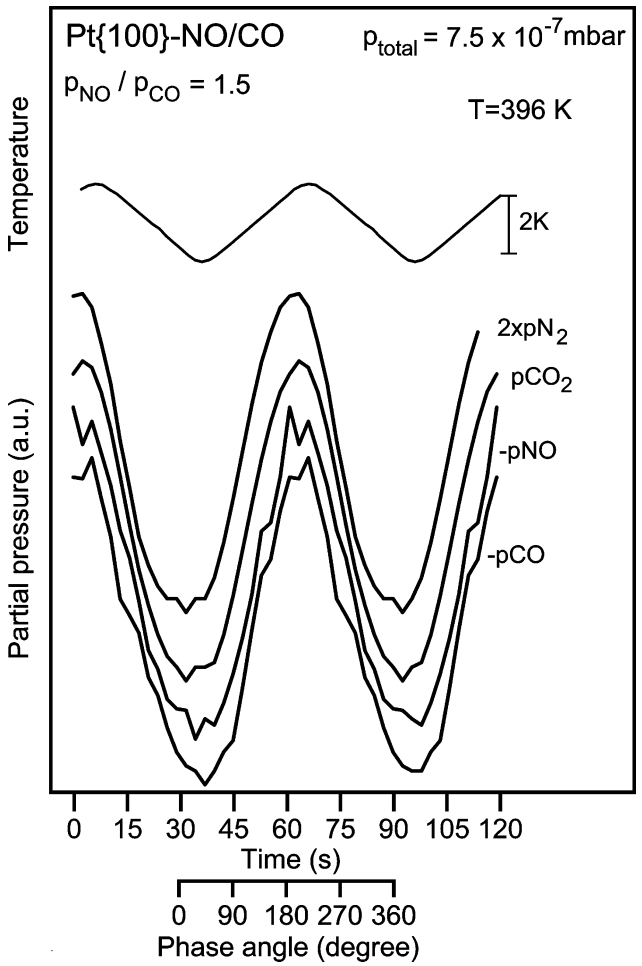

Figure 7. The time dependence of individual peaks in the mass spectrometer signal during the CO/NO oscillatory reaction over Pt{100} resulting from the application of a $^{13}C^{18}O/^{14}N^{16}O$ mixture in the partial pressure ratio 1:2 at a total reactant pressure of 7.5×10^{-7} mbar, average temperature 396 K with an applied temperature modulation of 2 K. Each plot is the result of an average over 5 oscillations of 60 s, each point represents a 2.65 s segment of the oscillation with a time resolution of 5.3 s. Displayed, from top to bottom, are the relative partial pressures N_2 (multiplied by a factor of 2), CO_2, and the NO and CO partial pressures, the latter two multiplied by (−1).

7 shows the CO and NO partial pressures multiplied by −1, thus generating a signal which reflects the rates of CO and NO adsorption; furthermore, the partial pressure of N_2 is multiplied by 2 in Figure 7 to allow for the fact that the surface reaction takes the form CO + NO → CO_2 + $^1/_2N_2$. The estimated precision of these partial pressure plots is 5% of the maximum values for CO and NO (the oscillation amplitudes are only 0.4% of the total signal for these two reactants) and 1% for CO_2 and N_2. While the signal-to-noise ratios of these data of Figure 7 are clearly inferior to those of the partial pressure plots of Figure 6, the important conclusion to be drawn from the results of this additional experiment is that the pressure variations of NO and CO are essentially identical in amplitude and phase, so we may assume that the temporal variation of the partial pressure of CO is closely similar to that of NO shown in Figure 6.

In fact, plotted in the form of Figure 7, it is clear that the variations in partial pressure of all the gases are very similar, with only very small differences in relative phase of their oscillations. This result has two important implications. First, the close similarity in phase of the variations in N_2 and CO_2 partial pressures implies that the production of both gases is controlled by the same rate-limiting mechanism, presumably that of NO dissociation. This lack of phase difference is in clear disagreement with the model of Hopkinson and King, which predicts that the N_2 oscillations should lag those of CO_2 by a 90° phase difference ($^1/_4$ of an oscillation period) and be of a flatter, more extended form.[11] In this regard the data are, however, consistent with the assumption of Fink et al. [9] that the formation of N_2 is immediate upon NO dissociation. On the other hand, the fact that the rate of reactant adsorption is very similar to the rate of product formation implies that the majority of the reaction occurs almost immediately on adsorption, i.e., that NO and CO adsorb on a cleared area of the surface, and immediately react. This process correlates with stage III of the oscillatory cycle (Figure 1), whereas in the model of Fink et al., the highest rate of reaction occurs due to the surface explosion and the reactive removal of the adsorbed layer, which is identified as the earlier stage II of the reaction cycle. Careful inspection of the data of Figure 7 suggests that the two product oscillations do appear to lead slightly those of the reactant gas pressures by about 2−3 s; bearing in mind that the pressures used correspond to a rate of arrival of gas molecules of each

species at the surface of very approximately 0.5 ML/s, this is consistent with the idea that the reactant consumption is governed by the creation of free sites by surface reaction. We should, however, beware of reading too much into such subtle details, as it is clear from the higher-quality partial-pressure data of Figure 6 that there are subtle variations in the shape of the temporal variations relative to the essentially sinusoidal variations which appear to dominate the data of Figure 7.

Consider now, the information provided by the IRAS data in terms of temporal variations of surface coverage. One interesting question is whether these data show any evidence for the role of nonreactive displacement of adsorbed NO by CO during the oscillatory reaction. We have already remarked that there is ample evidence that this replacement process does occur in coadsorption studies; it can be attributed to the higher heat of CO adsorption, as first proposed by Hopkinson and King,[11] but this process is not included in the modeling of the interaction by Fink et al.[9] The data of Figure 6 show that during the first 20 s or so of the oscillatory cycle (emboldened in Figure 6 and starting at a time of 30 s), the absorbance of the N−O IR band falls steadily, those of the C−O IR bands rise, yet the rate of CO_2 production remains low and the NO partial pressure actually rises very slightly. This combination of events can only be understood in terms of nonreactive displacement of NO by CO, so it is clear that this process *does* play a significant role in part of the oscillatory cycle. By contrast, however, coadsorption studies also show that NO cannot displace adsorbed CO in this way, so one may conclude that loss of surface CO is a direct measure of surface reaction. Using this fact, one can calculate a minimum value for the throughput of one oscillatory cycle as being the variation in coverage of atop CO. To do so we must relate the measured IR integrated absorbances to absolute coverages, and the data of Martin et al.[23] provide a basis for this calibration. Notice that as the isolated CO species giving the 2085 cm^{-1} wavenumber band does not contribute to the reaction, we ignore this component in the calculation. In particular, at 90 K and a coverage of 0.5 ML corresponding to a c(2 × 2) long-range ordered surface, they see essentially the same ratio of integrated absorbances of the bridge-to-atop bands, with both bands showing an integrated absorbance a factor of 3 larger than the peak values of our data. We therefore conclude that the maximum total (reactive) CO coverage during the reaction would be approximately $^1/_6$ ML if these species were distributed over the whole surface. However, we may estimate that approximately 20% of the surface is occupied by the nonreacting pure CO islands, so the peak coverage in the reacting area is approximately 0.20 ML. During the reaction, this value falls by a factor of 3, so the total amount of CO consumed in one cycle is approximately 0.13 ML. This value is consistent with estimates based on the measured changes in partial pressures in the gas phase, calibrated using thermal desorption of a known coverage of 0.5 ML of CO.

Figure 8 compares the partial pressure of CO_2 and the integrated absorbance of the NO, mixed atop CO, and bridged CO taken from Figure 6 (solid lines) with the predicted CO_2 yield and NO and CO surface coverages of the model of Fink et al. (shown schematically in Figure 1).[9] Of course, to make this comparison, it is necessary to determine the relative phases of the experimental and theoretical results; this has been achieved by aligning the centers of the main CO_2 partial pressure peaks in the two data sets. The exact shapes of these peaks in the experiment and theory differ, so there is some ambiguity in this alignment. In considering this comparison, it is therefore not possible to draw detailed conclusions from small phase

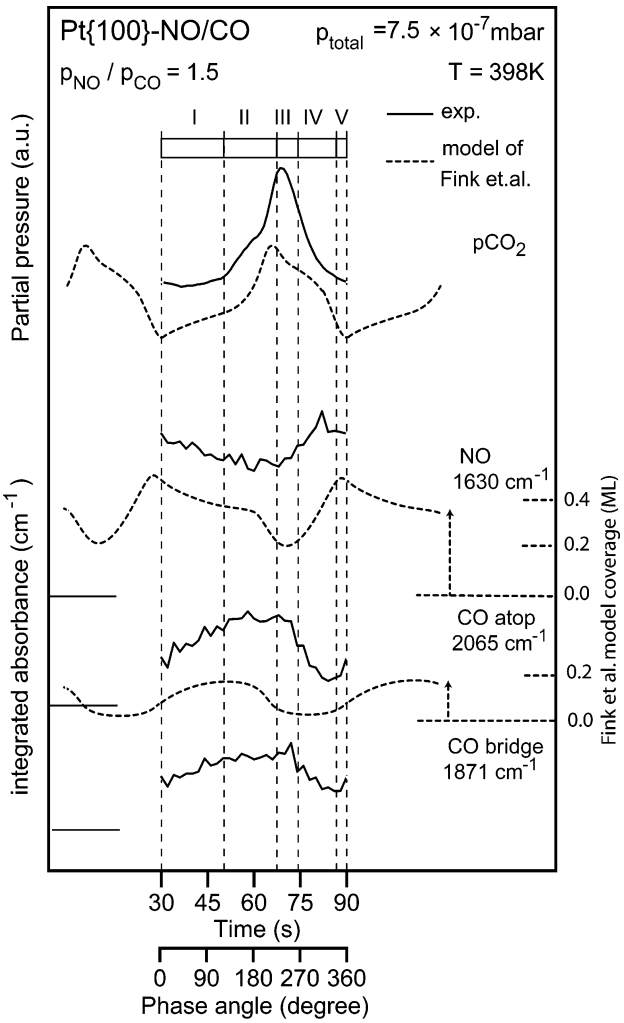

Figure 8. The time dependence of the CO_2 partial pressure and the absorbance of the three main IR bands (N−O, C−O atop, C−O bridge) during an oscillatory cycle, corresponding to the experiment of Figure 4. The dashed curves are the predictions of the CO_2 production and NO and CO surface coverages given by the model of Fink et al.[9] The roman numerals refer to the five stages of this model of the reaction shown schematically in Figure 1. The relative phases of the experimental and theoretical results have been adjusted to align the main peaks in the rate of CO_2 production. The horizontal lines correspond to zero values of integrated absorbance or coverage of the individual plots indicated by the vertical arrows. On the basis of the calibration methods described in the text, the estimated maximum coverages of CO and NO represented by the integrated absorbance plots are 0.20 and 0.36 ML respectively.

differences in the experimental and theoretical curves, although differences in the relative phases of two plots in theory and experiment should be meaningful.

Clearly the overall trends of the theoretical predictions and experimental measurements shown in Figure 8 are very similar. In particular, the relative phase of the variations of the partial pressure of CO_2 and the coverages of NO and CO on the surface during the oscillatory cycle are in excellent agreement with the model predictions, and many aspects of the shapes of the temporal variation of the CO coverage and CO_2 partial pressure are also in agreement. The actual surface coverages of NO and CO are also in rather good agreement with the model predictions. Figure 8 shows the predicted coverages explicitly, but the experimental integrated absorbances have not been converted to coverages and only the locations of the respective zero absorbances are marked on Figure 8 to allow comparison of the relative amplitudes of the variations. We have already shown,

however, that the peak coverage of reactive CO (both intermixed atop and bridging) is estimated to be 0.20 ML, in almost perfect agreement with the model prediction. A similar calibration of the N−O-integrated absorbance using spectra of the room-temperature saturation coverage of NO (in the absence of CO)[12] with an estimated coverage of 0.5 ML[21] allows us to convert the average integrated N−O absorbance of 0.07 cm^{-1} (Figure 6) to a coverage of 0.32 ML, similar to, but slightly less than, the predicted value of approximately 0.38 ML. Note, however, that the magnitude of the measured temporal variations of both the CO and NO coverages estimated from the IR absorbances are somewhat less than those seen in the model predictions; we will return to this aspect below.

Despite this excellent overall agreement, there are some significant differences in detail between theory and experiment. Notice, in particular, that in the experimental data, the minimum of the NO coverage, as determined by the absorbance of the N−O absorption band, occurs before the maximum in CO_2 production, whereas the order is reversed in the model predictions. This confirms our previously published result, recorded at lower spectral resolution[15] in an earlier report, it was suggested that the IRAS showed some evidence of an unresolved second N−O band which may correspond to a second species not considered in the existing model. However, the new higher-resolution spectra presented here show no evidence of such a component. Notice, too, that the experimental data show the NO surface coverage rising most steeply at a time in the cycle at which the CO surface coverage is falling most steeply; in the model predictions the CO coverage is almost constant and has a very low value at the equivalent point in the cycle.

In consideration of the origins of these discrepancies, we should note that our data clearly show the presence of bridging CO as well as atop CO on the surface, whereas no distinction between two sites is included in the model, so one might speculate that a different reaction of these two species with surface NO may play a role. However, the data clearly show that the variations of the integrated absorbance of these two species throughout the periodic cycle are essentially identical. A more reasonable explanation for the detailed discrepancies is that the model of Fink et al. fails to include the effect of the nonreactive displacement of NO by CO. The rate of this displacement process has not been determined at 400 K, but at 390 K, with equivalent partial pressures of NO and CO, CO was found to displace 50% of the NO coverage in 30 s;[12] evidently this process should be very significantly faster at 400 K, ensuring that it is important in an oscillatory process with a period of approximately 60 s. We have already shown that this displacement process can account for the fall in NO coverage and rise in CO coverage at the beginning of the oscillatory cycle of Figure 8 when the rate of CO_2 production is low (and not increasing as in the model predictions). The NO coverage can only increase by the reactive removal of CO, which creates free sites on the surface for NO adsorption; such free sites are preferentially occupied by NO because the NO partial pressure is higher than that of CO, and their sticking factors at such sites are both essentially unity. Indeed, the experimental data show that this point in the cycle, when the CO coverage starts to fall and the NO coverage starts to rise, corresponds to the highest reaction rate; in the experiment, therefore, the evidence is that this maximum rate arises from adsorption and immediate reaction. By contrast, the model of Fink et al. shows the highest reaction rate resulting from the surface explosion, which occurs when the surface coverage of CO and NO are falling steeply simultaneously.

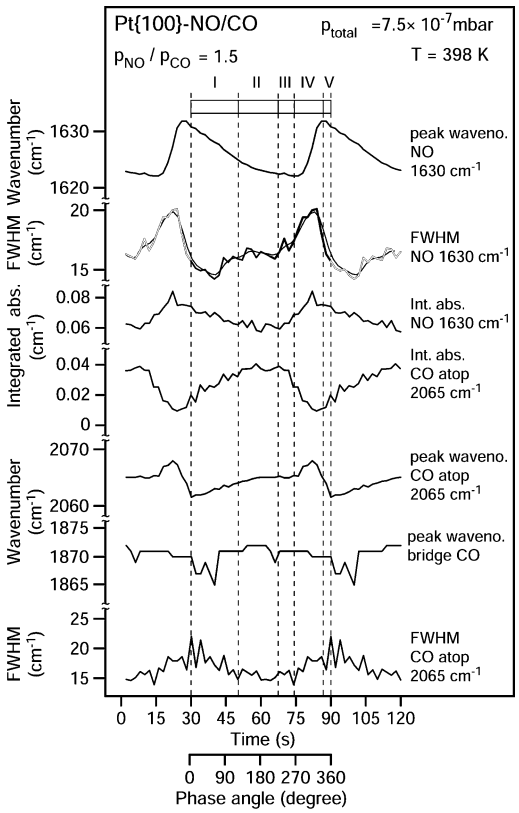

Figure 9. The time dependence of the peak wavenumber, fwhm, and integrated absorbance of the three main IR bands (N−O, C−O atop, C−O bridge) during an oscillatory cycle, corresponding to the experiment of Figure 4. The dashed curves are the predictions of the CO_2 production and NO and CO surface. The roman numerals refer to the five stages of the reaction according to the model of Fink et al.[9] shown schematically in Figure 1 aligned in phase as in Figure 8.

In view of the fact that the surface explosion lies at the heart of the model of Fink et al., this discrepancy at first appears rather serious. However, our comparison of theory and experiment is based on the assumption that the experiment (like the theory) corresponds to conditions in which the surface is homogeneous and changes in the surface coverage with time are perfectly synchronous. While the general methodology adopted here is designed to ensure that this is basically correct, we know that in this bistability the major transformation of the surface occurs by the propagation of a reaction front, so at some points in the cycle there must be local inhomogeneity. Clear evidence that this is the case is contained in the variation of the exact frequencies and widths of the IRAS absorption bands through the periodic cycle, and these are shown, together with the band absorbances, in Figure 9. We should recall that the main factor influencing the exact frequencies of the N−O and C−O stretching bands is dynamic dipole coupling, so higher *local* coverages of a single species lead to higher frequencies. There are also contributions from so-called chemical shifts in which the vibrational frequency is influenced by modified electronic interaction with the surface due to coadsorbed atoms and molecules (including those of the same species) but these effects are known to be small for CO and NO on Pt surfaces. Bearing this in mind, one particularly striking aspect of the data of Figure 9 is that the peak wavenumber of the intermixed atop C−O stretching mode around 2065 cm^{-1} displays a sharp maximum at the point in the cycle at which the integrated absorbance of this band is minimum. In effect, therefore, this implies that the *local* coverage of this species is greatest at the condition when the *average* coverage is lowest. Clearly this

can only be reconciled with two different spatially separated states on the surface. Notice too that this occurs at a point in the cycle at which the average coverage of NO reflected by the N−O absorbance is high (essentially maximum), but the full width at half-maximum (fwhm) of this N−O band also shows a narrow peak. The most obvious interpretation of this is that there is a significant NO coverage in both the states of the surface, but the local NO coverages in these two states differ, leading to a kind of inhomogeneous broadening (or two nearby unresolved components). Notice, incidentally, that the time dependence of the N−O stretching frequency has an overall form which is quite similar to that of its integrated absorbance, indicating that the local and average NO coverages are similar over most of the cycle, although the frequency rises more sharply than the absorbance in the same part of the cycle we have now identified with a two-phase regime, also consistent with differences between local and average coverage. These results therefore indicate that in the section of the reaction cycle labeled IV, reaction fronts are moving over the surface, transforming it from a state of relatively high CO coverage and low NO coverage, to one of relatively low CO coverage and high NO coverage.

We should perhaps also remark that one consequence of this kind of asynchronous transformation of the surface is that the experiments measure average coverages over the two-phase region, so one might expect that the experimental coverage variations would be smaller than those predicted for homogeneous surface transitions. This may account, at least in part, for the reduced modulation amplitudes which we have remarked upon.

3.3. The Role of the Bridging CO Species. So far we have discussed the reaction almost entirely in terms of the atop CO species corresponding to the 2065 cm^{-1} IRAS band, although in addition to the "spectator" atop CO species (2085 cm^{-1} IRAS band), which clearly does not participate in the reaction, we also see a bridging CO species (1875 cm^{-1} IRAS band). Models of the NO/CO reaction over Pt{100} have assumed that only one CO species is present, but the variations of the integrated absorbance of the bridged species through the reaction cycle clearly shows that these CO species are involved in the reaction in some way. We must therefore consider whether the presence of this bridging CO plays an important role in the reaction. Of course, the similarity of the variations of the integrated absorbance of the bridging and intermixed atop CO species during the reaction cycle (Figure 6) shows that at least some of these species must clearly be intermixed with the NO on the surface, and not in isolated islands as in the case of the 2085 cm^{-1} atop CO species. In view of the fact that we have shown that there are two distinct atop CO states, however, one in pure CO islands and one intermixed with (and reacting with) NO, we might ask whether the same is true for the bridging CO. Notice that the bridging C−O band is weaker and broader than the atop C−O band, so it is not possible to establish whether there is any significant splitting of this band. However, if we compare the changes of integrated absorbance of the bridge C−O band through the reaction cycle we find that it displays a very similar behavior to that of the *sum of both atop* C−O bands. The minimum absorbance of the bridged C−O band is 52 ± 5% of its maximum value, similar to the value of 60 ± 2% for the total intensity of both atop species and quite different from the value of 30 ± 3% for the intermixed (2065 cm^{-1}) atop C−O band alone. Furthermore, whereas the ratio of the integrated absorbance of the bridged and *both* atop C−O bands has an approximately constant value of 0.26 ± 0.06 thoughout the oscillatory cycle, the average value of the ratio of the integrated absorbance of bridged C−O to the intermixed component of the atop C−O absorption band alone is 0.51 and varies between 0.81 and 0.42. These comparisons show rather clearly that there are two bridged CO species, one intermixed with NO and involved in the reaction and one that is in pure CO islands which are not involved in the reaction. This conclusion is consistent with independent steady-state coadsorption IRAS measurements[12] in which the presence of bridged CO in both environments is also observed. Notice that the almost constant value of the ratio of the integrated absorbance of the bridged C−O to the sum of the two atop C−O absorption bands is indicative that the relative proportions of the bridged and atop CO species is similar in both NO-intermixed and pure CO environments is similar; this result is also consistent with IRAS studies of the transient behavior of the coadsorption system when subjected to thermal steps.[12] On the basis of the conclusions of the earlier study of pure CO on Pt{111},[23] it seems that the inactive bridged CO species must occur in pure bridged CO islands which coexist with the "spectator" atop CO islands responsible for the IR absorption band at 2085 cm^{-1}.

In considering the role of the intermixed bridged CO in the NO/CO reaction, one further important observation is that previous studies of coexistent atop and bridged CO on this surface have shown that there is a high rate of interchange between bridged and atop CO at these temperatures, the relative occupation of the two species being in equilibrium.[23] This same effect has also been shown to occur in the NO/CO coadsorption situation in which the NO and CO are intermixed on the surface, although these studies also show that in the nonreactive displacement of NO by CO, the actual displacement is effected by atop CO.[12] In particular, it has been shown, at 390 and at 300 K (both temperatures below that at which CO/NO reaction occurs), that if a surface which is initially NO covered is exposed to CO, CO adsorption occurs at first in the atop site but with subsequent occupation of bridge sites. At 390 K under similar conditions to those used in this experiment, there is a 9.0 ± 4.5 s lag between the exposure of CO to NO + Pt{100} and the equilibration between bridged and atop CO. At the slightly higher temperatures of the oscillatory reaction investigated here, this delay time will be significantly shorter. Strictly, the fact that the nonreactive displacement of NO is effected by only atop CO does not necessarily mean that only atop CO is involved in the reactive removal of NO, but the rapid equilibration between the two CO species means that which species (if indeed it is only one species) is involved in the reaction will have little significance in influencing the behavior of the oscillatory reaction cycle.

4. Conclusions

Overall, the results of our measurements of the temporal variation of the CO and NO surface coverages, and the rate of reactant uptake and product generation, are in very good agreement with predictions of the model proposed by Fink et al.,[9] although there are some detailed discrepancies. We attribute many of these differences to two factors: (1) the fact that even in an experiment designed to maintain a homogeneous surface with synchronous changes in the state of the whole surface, some transformations (such as the surface explosion) inevitably involve reaction front propagation and thus inhomogeneity and (2) the neglect in the model of the process of nonreactive displacement of NO by CO.

Our results also show that two CO species, atop and bridged, are involved in the reaction within the intermixed NO + CO

regions of the surface. Although this factor has not been considered in previous models of the reaction, bridged CO is shown to play an equivalent role in the reaction mechanism to atop CO, primarily because the two species rapidly equilibrate with one another. For this reason, it is sufficient that a model simply consider "adsorbed CO". Somewhat surprisingly, the coexistence of nonreacting pure atop CO islands is also observed (and coexistent nonreacting pure bridge CO islands are also inferred). The extent to which these "spectator" islands occur appears to be very sensitive to the exact experimental conditions and appears to be favored at the lowest temperatures of the "low-temperature" oscillatory reaction regime at which the rate of NO dissociation is probably only just sufficient to sustain the reaction.

Clearly it would be of interest to extend the model of Fink et al. to include the mechanism of nonreactive replacement of NO by CO and make a more detailed comparison of the results with our experimental data. It may, however, be even more fruitful to go beyond a mean-field model (such as that used by Fink et al.[9] and Hopkinson and King).[11] In particular, advances in the time-dependent (dynamic) Monte Carlo[32,33] simulation of kinetic oscillations in heterogeneous catalytic systems can be extended to predict pattern formation, as has been successfully performed for the CO oxidation reaction by Gelten et al.[34] An improved model of the CO + NO reaction system might be achieved by extending the lattice-gas model of Tammaro and Evans[10] of the surface explosion to include both the adsorption, from an applied partial pressure of both gases, and the displacement of NO by CO. This would allow modeling of the stages of the oscillatory cycle after the surface explosion, and the resulting spatio-temporal model may then reproduce the various pattern formation observed by PEEM and LEEM as well as our own experimental results.

References and Notes

(1) Hugo, P. *Ber. Bunsen-Ges., Phys. Chem.* **1970**, *74*, 121.
(2) Beusch, H.; Fieguth, P.; Wicke, E. *Chem. Ing. Tech*. **1972**, *44*, 445.
(3) Scheintuch, M.; Schmitz, R. A. *Catal. Rev. Sci. Eng.* **1977**, *15*, 107.
(4) Ertl, G. *Adv. Catal*. **1990**, *37*, 213.
(5) Imbihl, R. *Prog Surf. Sci.* **1993**, *44*, 183.
(6) Veser, J.; Imbihl, R. *J. Chem. Phys.* **1994**, *100*, 8492.
(7) Schüth, F.; Wicke, E. *Ber. Bunsen-Ges. Phys. Chem.* **1989**, *93*, 191.
(8) Singh-Boparai, S. P.; King, D. A. In *Proceedings of the Fourth International Conference on Solid Surfaces and the Third European Conference on Surface Science*; Degras, D. A., Costa, M., Eds.; SFV: Paris, 1980.
(9) Fink, Th.; Darth, J.-P.; Imbihl, R.; Ertl, G. *J. Chem. Phys.* **1991**, *95*, 2109.
(10) Tammaro, M.; Evans, J. W. *J. Chem. Phys.* **1998**, *108*, 7795.
(11) Hopkinson, A.; King, D. A. *Chem. Phys.* **1993**, *177*, 433.
(12) Miners, J. H.; Gardner, P.; Woodruff, D. P. *Surf. Sci.*, submitted.
(13) Yeo, Y. Y.; Vattuone, L.; King, D. A. *J. Chem. Phys.* **1996**, *104*, 3810.
(14) Willis, H. A.; Powell, D. B. In *Perspectives in Modern Chemical Spectroscopy*; Andrews, D. L., Ed.; Springer-Verlag: Berlin, 1990.
(15) Miners, J. H.; Martin, R.; Gardner, P.; Nalezinski, R.; Bradshaw, A. M. *Surf. Sci.* **1997**, *377*−*379*, 791.
(16) Magtoto, N. P.; Richardson, H. H. *Surf. Sci.* **1998**, *417*, 189.
(17) Miners, J. H.; Gardner, P. *J. Phys. Chem. B* **2000**, *104*, 10265.
(18) Dath, J.-P.; Fink, Th.; Imbihl, R.; Ertl, G. *J. Chem. Phys.* **1992**, *96*, 1582.
(19) Veser, J.; Mertens, F.; Mikhailov, A.; Imbihl, R. *Phys. Rev. Lett.* **1993**, *71*, 935.
(20) Gardner, P.; Tüshaus, M.; Martin, R.; Bradshaw, A. M. *Vacuum* **1990**, *41*, 385.
(21) Gardner, P.; Martin, R.; Tüshaus, M.; Bradshaw, A. M. *Surf. Sci.* **1990**, *240*, 122.
(22) Gardner, P.; Martin, R.; Tüshaus, M.; Bradshaw, A. M. *J. Electron. Spec. Relat. Phenom.* **1990**, *54*/*55*, 619.
(23) Martin, R.; Gardner, P.; Bradshaw, A. M. *Surf. Sci.* **1995**, *342*, 69.
(24) Crossley, A.; King, D. A. *Surf. Sci.* **1980**, *95*, 131.
(25) Banholzer, W. F.; Masel, R. I. *Surf. Sci.* **1984**, *137*, 339.
(26) Gardner, P.; Martin, R.; Tüshaus, M.; Bradshaw, A. M. *Surf. Sci.* **1992**, *269*, 405.
(27) Seebauer, E.; Schmidt, L. *Chem. Phys. Lett.* **1986**, *123*, 129.
(28) Kwasniewski, V.; Schmidt, L. *Surf. Sci.* **1992**, *274*, 329.
(29) Norton, P. R.; Davies, J. A.; Creber, D. K.; Sitter, C. W.; Jackman, T. E. *Surf. Sci.* **1984**, *108*, 205.
(30) Norton, P. R.; Binder, P. E.; Griffiths, K. *J. Vac. Sci. Technol., A* **1984**, *2*, 1028.
(31) Zemlyanov, D. Y.; Smirnov, M. Y.; Gorodetskii, V. V.; Vovk, E. I. *Catal. Lett.* **1997**, *46*, 201.
(32) Gillespie, D. T. *J. Comput. Phys.* **1976**, *22*, 403.
(33) Gillespie, D. T. *J. Phys. Chem.* **1977**, *81*, 2340.
(34) Gelten, R. J.; Jansen, A. P. J.; Van Santen, R. A.; Lukkien, J. J.; Segers, J. P. L.; Hilbers, P. A. J. *J. Chem. Phys.* **1998**, *108*, 5921.